*32nd EPS Conference on Plasma Phys. Tarragona, 27 June - 1 July 2005 ECA Vol.**29C**, D-4.007 (2005)*

First observation of ETG mode component of tokamak plasma turbulence by correlative UHR backscattering diagnostics

E.Z. Gusakov, A.D. Gurchenko,

A.B. Altukhov, A.Yu. Stepanov, L.A. Esipov, M.Yu. Kantor, D.V. Kouprienko

Ioffe Physico-Technical Institute, 26 Polytekhnicheskaya st., St.-Petersburg, Russia

Electrostatic fine scale electron temperature gradient (ETG) mode turbulence is discussed nowadays as a possible candidate for explanation of the anomalous electron energy transport in tokamak plasmas, especially in transport barriers [1-5]. According to theoretical and computational analysis of [1, 2], performed using gyrokinetic approach in flux tube geometry, this turbulence, possessing shortest wave length in the electron gyroradius range, can nevertheless cause a substantial heat flux due to formation of streamers at the nonlinear stage of its evolution. On contrary, the global fluid simulations [3-5] have shown much smaller heat flux, which was explained by instability saturation at a lower level due to toroidal mode coupling. These contradictory theory predictions have not been checked yet experimentally, due to complications caused by extremely small scale of ETG modes. The attempt to address this problem using the upper hybrid resonance backscattering diagnostics (UHR BS) [6] is presented in this paper.

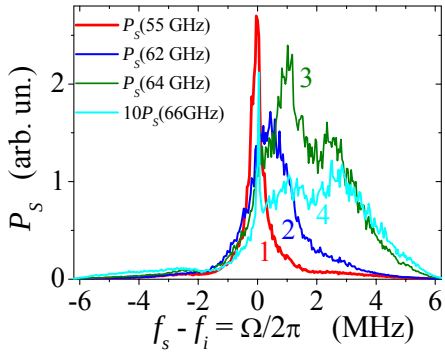

Fig. 1. *UHR BS spectra.* 1: r_{UH} = 7.9 cm; 2: 6 cm; 3: 5.6 cm; 4: 5 cm.

The experiment is performed at the FT-2 tokamak ($R = 55$ cm, $a = 8$ cm, $B_T \approx 2.2$ T, $I_p = 19 \div 37$ kA, $n_e(0) = (2 \div 4) \times 10^{19}$ m^{-3}, $T_e(0) \approx 500$ eV) where a steerable focusing double antennae set, allowing off equatorial plane plasma *X*-mode probing from high magnetic field side with maximal vertical displacement $y_a = \pm 2$ cm is installed. The beam radius at the UHR position, where the probing frequency (52 – 69 GHz) satisfies condition $f_i^2 = f_{ce}^2(R) + f_{pe}^2(r)$, is $\rho \approx 0.7 \div 0.9$ cm. The probing wave electric field, radial and poloidal wave number grows rapidly in the vicinity of the UHR, where the BS efficiency $S_{BS}(q_R)$ possesses sharp maximum [6, 7]. The diagnostics benefits of this growth leading to high localization, enhanced sensitivity to sub-millimeter scales and substantial frequency shift of the BS wave

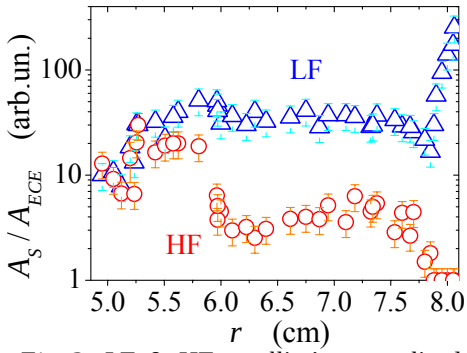

Fig. 2. *LF & HF satellite's normalized spectral amplitudes profiles.*

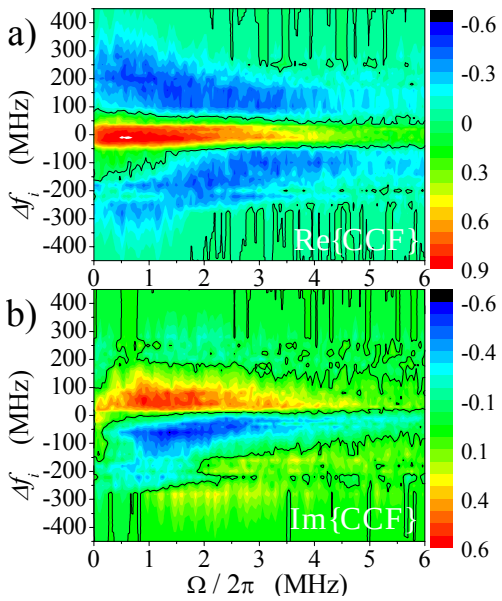

Fig. 3. *Normalized CCF for* $r_{UH} = 6.4$ cm.

(Enhanced Doppler effect) [8]. The probing wave UHR layer was situated at $r > 4$ cm, where condition for the ETG mode excitation [2] $L_T < 1.25\, L_n$ was fulfilled. The UHR BS spectra obtained in 32 kA ohmic discharge at different probing frequencies and, correspondingly, UHR positions are shown in fig. 1. The BS spectrum is weakly shifted and symmetric at the edge, whereas its shift and asymmetry grows, when moving inward. At $r_{UHR} = 5.6$ cm the second line possessing more than twice higher frequency shift appears in the spectrum. At $r_{UHR} = 5$ cm its amplitude exceeds the amplitude of the first line. The spatial distribution of their amplitude normalized to the ECE signal is shown in fig. 2. As it is seen, the amplitude of the low frequency (LF) satellite decreases when moving inward whereas the high frequency (HF) satellite's amplitude increases. The observation of a doublet in the UHR BS signal is most likely associated with simultaneous excitation of two different drift modes in FT-2 plasma. To check this supposition the wave number spectrum of turbulence was investigated with correlation technique [9]. Two BS signals at close probing frequencies with difference Δf_i, measured simultaneously were utilized for the cross-correlation function (CCF) computation. The normalized CCF obtained at the reference frequency 61.9 GHz in 32 kA discharge at $y_a = 1.5$ cm is shown in fig. 3 (a – real part; b – imaginary). The Δf_i width of the high coherency region there decreases with growing turbulence frequency Ω. As a result, the higher wave numbers q_R should correspond to higher Ω in the cross-correlation spectrum (CCS), obtained by Fourier transform from the CCF dependence on the UHR spatial separation, proportional to Δf_i. The corresponding CCS proportional to the product of density fluctuations spectral power density and $S_{BS}(q_R)$ is shown in fig. 4a. The imaginary part of the CCS (fig. 4b), which should be zero in theory,

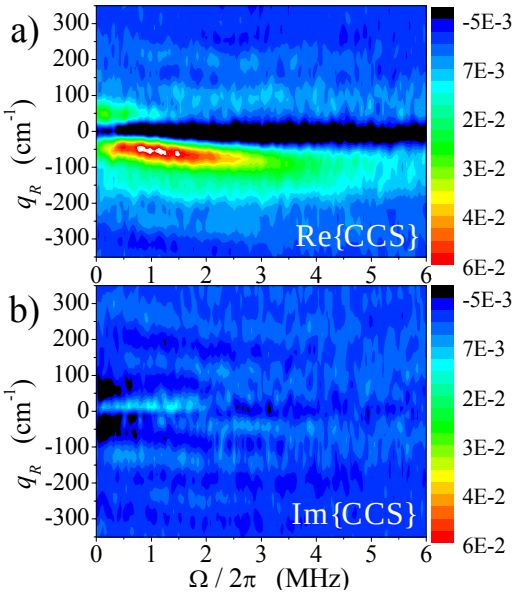

Fig. 4. *CCS for* $r_{UH} = 6.4$ cm.

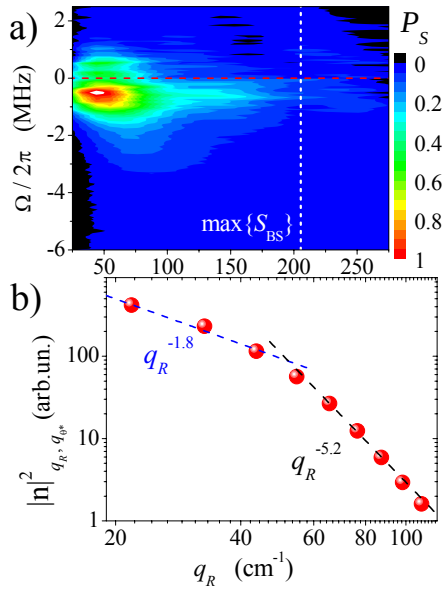

Fig. 5. *UHR BS signal spectrum* (a) *and turbulence wave number spectrum* (b) *for* 32 kA, 61.9 GHz (r_{UH} = 6.4 cm).

determines the accuracy of our procedures. The UHR BS spectrum, obtained from the CCS multiplying it by the signal frequency spectrum (integral in q_R), is shown in fig. 5a and fig. 6a for two extreme cases of dominating LF and HF satellites, correspondingly. The first case, in which low q_R in the interval 25 – 100 cm^{-1} and frequency less than 1 MHz are measured, is typical for the plasma edge. The second spectrum, where frequencies are higher than 2 MHz and q_R reach 250 cm^{-1} is never observed at the edge, but in the central region at $r < 5$ cm. To obtain the turbulence wave number spectrum $|n|^2_{q_R,q_\theta,\Omega}$ from these figures we supposed that the UHR BS spectrum is determined by the turbulence spectrum, BS efficiency, as well as by the antenna beam, and given by integral over poloidal wave number q_θ of fluctuations: $P_{BS}(q_R,\Omega) = \int |n|^2_{q_R,q_\theta,\Omega}\, S_{BS}(q_R) F^2(y) dq_\theta$, where the antenna beam power distribution in the vertical direction on the UHR is given by $F^2 = \exp\{-2(y-y_*)^2/\rho^2\}$. We also account for the relation [8] between q_θ of fluctuations contributing to the signal and vertical displacement of the point where it happens $q_\theta = 2k_{\theta*}(y/y_*) + q_R \cos\gamma_* (y/y_*)$ and nonlinear broadening of turbulence spectrum $|n|^2_{q_R,q_\theta,\Omega} = |n|^2_{q_R,q_\theta} \exp\{-(q_\theta - \Omega/V_\theta)^2/\Delta q_\theta^2\}\sqrt{\pi}/\Delta q_\theta$.

As a result of fitting, following parameters were obtained in the case of fig. 5a (32 kA): $V_\theta = 3.1$ km/s, $q_{\theta*} = q_\theta(y_*) = 13$ cm^{-1}, $\Delta q_\theta = 13$ cm^{-1}, $q_R^{max} = 50$ cm^{-1}. The turbulence q_R spectrum in this case is shown in fig. 5b in double logarithmic scale. It scales as $q_R^{-1.8}$ for $25 < q_R < 50$ cm^{-1} and as $q_R^{-5.2}$ for $50 < q_R < 100$ cm^{-1}. This behavior is similar to that observed on Tore Supra tokamak for ITG mode turbulence [10]. In the case of HF satellite of fig. 6a (22 kA) fitting parameters are $V_\theta = 2.5$ km/s, $q_{\theta*} = 64$ cm^{-1}, $\Delta q_\theta = 24$ cm^{-1}, $q_R^{max} = 160$ cm^{-1}. The turbulence q_R spectrum in this case is shown in fig. 6b. Its quick, as $q_R^{-5.7}$, decay at $50 < q_R < 180$ cm^{-1} saturates at higher wave numbers. The frequency of turbulence modes producing BS in this

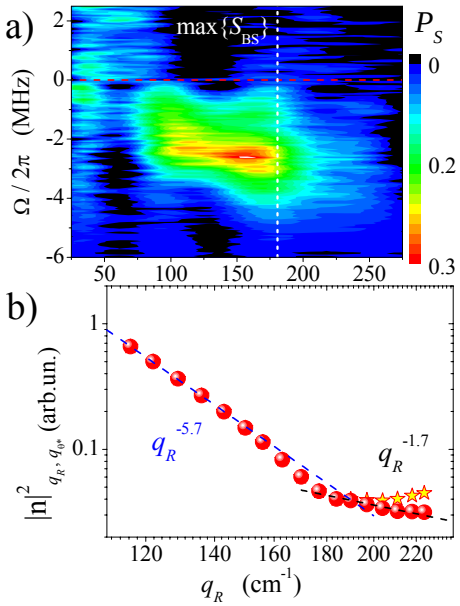

Fig. 6. *UHR BS signal spectrum* (a) *and turbulence wave number spectrum* (b) *for* 22 kA, 65.8 GHz (r_{UH} = 3.8 cm).

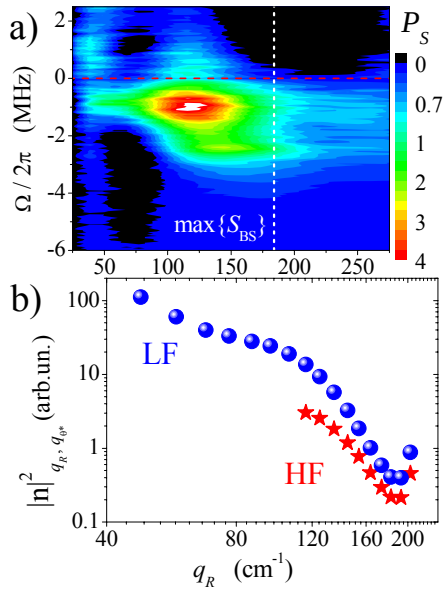

Fig. 7. *UHR BS signal spectrum* (a) *and turbulence wave number spectrum* (b) *for* 32 kA, 64.4 GHz (r_{UH} = 5.6 cm).

case are much higher than in fig. 5a as well as the range of wave numbers where they are observed is not usual for ITG or TEM mode. It is natural to associate this mode with the ETG mode which should be unstable under the experiment conditions. The parameters of these modes were directly compared in the experiment at 32 kA current, where they were observed simultaneously (fig. 7a). The LF satellite at 1 MHz is larger there than the HF satellite at 2.4 MHz, which possesses higher q_R. The fitting for these two satellites results in parameters: $V_\theta = 2.7$ km/s, $q_{\theta*} = 23$ cm^{-1}, $\Delta q_\theta = 19$ cm^{-1} for ITG mode and $V_\theta = 5.6$ km/s, $q_{\theta*} = 27$ cm^{-1}, $\Delta q_\theta = 10$ cm^{-1} for ETG mode. The huge excess of the HF mode phase velocity provides additional argument in favor for its physical difference. The turbulence q_R spectrum reconstructed for these modes is shown in fig. 7b.

Summarizing the results of the paper we would like to state that two modes are found in the UHR BS spectra under conditions when the threshold for the ETG mode instability $L_T < 1.25\, L_n$ is overcome. The first possessing frequency less than 1 MHz and radial wave number $25 < q_R < 150$ cm^{-1} is localized at the plasma edge and associated with the ITG mode. Its wave number spectrum is quickly decaying in the way similar to that observed at Tore Supra. The second possessing frequency higher than 2 MHz and radial wave number $q_R > 150$ cm^{-1} is associated with the ETG mode. Its phase velocity is twice as high and amplitude is growing towards the centre. In the region of observations its level is comparable to that of the ITG mode, been however much smaller than the later one at the edge.

Financial support of RFBR grants 04-02-16534, 05-02-16569, scientific schools state program HIII-2159.2003.2, INTAS grant 01-2056 and NWO-RFBR grant 047.016.015 is acknowledged.

1. F. Jenko, W. Dorland, M. Kotschenreuther, B.N. Rogers, Phys. Plasmas 7, 1904 (2000).
2. F. Jenko, W. Dorland, G.W. Hammett, Phys. Plasmas 8, 4096 (2001).
3. B. Labit, M. Ottaviani, Phys. Plasmas 10, 126 (2003).
4. J. Li, Y. Kishimoto, Phys. Plasmas 11, 1493 (2004).
5. Z. Lin, et al., IAEA-CN/TH/8-4 (2004).
6. K.M. Novik and A. D. Piliya, Plasma Phys. Control. Fusion 35 ,357 (1993).
7. D.G. Bulyiginskiy, A.D. Gurchenko, E.Z. Gusakov, et al., Phys. Plasmas 8, 2224 (2001).
8. A.B. Altukhov, et al., 30 EPS Conf. on Control. Fusion and Plasma Phys. ECA 27A (2003), P-4.170pd.
9. E.Z. Gusakov, et al., 42, 1033 (2000).
10. P. Hennequin, et al., Plasma Phys. Control. Fusion 46, B121 (2004).